An Investigation into the Effect of Post-Veraison Irrigation Regimes on Late-Season Dehydration in *Vitis Vinifera* cv. Cabernet Sauvignon Berries

By

ALEXANDER J RITTER-JENKINS
THESIS

Submitted in partial satisfaction of the requirements for the degree of

MASTER OF SCIENCE

in

Viticulture & Enology

in the

OFFICE OF GRADUATE STUDIES

of the

UNIVERSITY OF CALIFORNIA

DAVIS

Approved:

Megan K. Bartlett, Chair

Dario Cantù

Andrew J. McElrone

Committee in Charge

2024

## Table of Contents

## Acknowledgements

In the context of a graduate program aimed at preparing students for the wine industry, I thank Dr. Megan Bartlett for not only the opportunity to study an important topic with practical importance in winemaking and viticulture, but also her diligence and accessibility throughout that helped move this project along efficiently. She kept my spirits high and provided reassurance when I needed it.

In addition to sharing with me his technical prowess in microscopy, Post-doctoral researcher Ryan Stanfield helped me think and plan lab work like a scientist. Thank you to my lab mate Gabriela Sinclair, who supplied many silver bullets of knowledge that saved me many precious hours of labor, and to Tianle Gao for his perseverance in braving the Davis summer heat with me during midday water potentials. I greatly appreciated Rosa Figueroa Balderas and Melanie Massonnet of the Cantu Lab for their time and support in various laboratory analyses.

I am also grateful for Guillermo Garcia Zamora for his consultations on experimental design, and special thanks to Jovita of the UCD vineyard team for helping me install irrigation lines.

Finally, I must express gratitude for my fellow graduate classmates who immensely enriched my experience at Davis and were always there to remind me of what makes wine worth studying.

## Abstract

Late season dehydration (LSD) is a type of berry shrivel in wine grapes occurring at the end of ripening as a result of cell death in the mesocarp of mature berries and is accelerated by late season water deficits. Increasing temperatures and erratic precipitation are projected for California's winegrowing regions this century, rendering grapevines more vulnerable to late season dehydration and consequently growers to yield losses. This study sought to investigate whether augmented volumes ('pulses') of irrigation prior to (the early treatment) or during (the late treatment) the onset of cell death would effectively postpone it. Water potential and gas exchange measurements were compared to mesocarp cell death, degree of berry shrivel, and chemical agents and products of cell death. Our study found that a 40% difference in irrigation volume for our pulses did not effect changes in water potential, stomatal conductance, or photosynthesis, however the late treatment significantly slowed the rate of cell death and yielded more turgid berries at harvest. Other aspects of berry quality, at harvest, (°Brix, TA, pH) did not respond to our treatments. We observed a spike in $H_2O_2$ at the onset of cell death and found significant correlation between tissue vitality and $H_2O_2$ concentrations throughout the experimental period. Thus, our study confirmed the relationship between H2O2 accumulation and berry shrivel, and found a potential irrigation strategy for mitigating LSD-related yield losses. A complete picture of the mechanism of LSD is needed to fully explain how shrivel responds to irrigation: future studies on this topic could provide an account of water dynamics in the berry in relation to cell death and irrigation by additionally monitoring hydraulic conductivity in the pedicel. Further investigation into transcriptional changes before and during the onset of cell death will also be needed to determine the contribution of programmed cell death late in berry development.

## Introduction

*The Problem of Late Season Dehydration*

The Mediterranean growing conditions of California's wine regions, characterized by wet winters and hot dry summers, are predicted to be exacerbated by climate change within this century. These conditions require irrigation to meet target yields and achieve desired grape quality for winemaking. Warming trends since 1880 have caused consistent increases in temperatures in California that are projected to continue through the next century, with the number of hot (>95°F) days predicted to increase by up to three weeks by 2040 (Livneh et al. 2015; Rasmussen et al. 2016). Consequently, climate change has increased the frequency of extreme weather events, with northern coastal regions being the second the most effected by heatwaves in the California (Gershunov and Guirguis 2012). Precipitation in California is projected to increase, on average, but become more variable, rendering vineyard land more vulnerable to drought in dry years, especially in the face of increasing restrictions on using groundwater for irrigation (Swain et al. 2018). Vineyard land that relies on snowpack from the Sierras for irrigation will also become more vulnerable to drought, as the snowpack supply for all of the western United States has been projected to diminish by 60% in the next 30 years (Fyfe et al. 2017; Berg and Hall 2017). Given the likelihood of increasing drought conditions and water restrictions for winegrowers throughout the state, the judicious use of irrigation will become paramount to mitigating impacts on yield and wine quality.

One issue affecting ripening grapes in Mediterranean regions that reduces yield, affects berry quality, and has been linked to plant water stress is late-season dehydration (Keller, 2010; Bonada et al. 2013b; Chou et al. 2018; Bondada et al., 2017). Late-ripening *Vitis vinifera*

cultivars, which constituted at least 29% of 2022 California Crush (i.e. Zinfandel, Cabernet Sauvignon, Cabernet Franc, Petite Verdot, Petite Syrah and Syrah), are especially susceptible to late season dehydration (LSD) due to changes in climate and winemaking styles (CDFA 2022). Harvested as late as October-November, their ripening has traditionally occurred in cooler fall months during which, now, we observe warmer temperatures. Despite evidence that anthropogenic greenhouse gases have pushed forward grape harvests throughout the world, one would be wrong to assume that overall warmer temperatures have caused these grapes to be harvested significantly earlier (Webb et al. 2012, Cook et al. 2016). Stylistically, there has been a shift in the desired characteristics of wines that necessitates extended hangtime (Alston et al. 2011). For example, the average °Brix at harvest for Cabernet Sauvignon in California has increased from 22.0 in 1975 to 25.2, and similar trends exist for total red and white grapes (Alston et al. 2011; CDFA, 1975-2023). Such lengthened ripening periods leave grapes more vulnerable to LSD, likely requiring additional irrigation to compensate (especially in the face of heatwaves and drought).

*Effects on Fruit Composition and Wine*

The consequences of LSD for winemakers concern the chemical as well as sensory properties of berries and wine. The progression of LSD is strongly correlated to the overall flavor intensity of Syrah grape berries (Bonada et al. 2013a; Bonada et al., 2015). While that may be a favorable outcome with respect to wine quality, LSD also staggers the development of seed tannin (accelerated) and skin/pulp attributes (relatively delayed), two sensory properties winemakers often rely on to gauge overall fruit maturity (Bonada et al., 2013a). Furthermore, for red wine grapes, shriveled berries can cause dramatic shifts in °Brix once in tank, requiring unexpected

must treatment and reducing overall predictability of initial conditions for fermentation. In terms of berry chemistry, LSD-stricken berries have lower tartaric and malic acid concentrations, and higher calcium and potassium concentrations, all of which can increase the likelihood of unwanted fungal/bacterial growth during fermentation (Bondada and Keller, 2012; Bondada et al., 2017).

In the vineyard, LSD can cause yield losses between 10-30% with the greatest losses occurring in vulnerable cultivars like Syrah (Keller, 2010; Tilbrook and Tyerman, 2009; Rogiers and Holzapfel, 2015). While fruit shrivel of any kind reduces yield, LSD is one of the better understood forms of shrivel in terms of developing prevention strategies compared to the nebulous genetic disorders Bunch Stem Necrosis and Sugar Accumulation Disorder (SAD). Sunburn shrivel is commonly solved through shade cloth and cultural practices whereas for LSD, irrigation has been the go-to strategy attempted by growers as well as the main target of research concerning this problem.

In quantifying the effects of LSD experimentally, cell vitality, correlated with LSD shrivel in 22 grape cultivars (Fuentes et al., 2010), has been measured in berries as a response to varying levels of abiotic stress. Syrah berries were observed to undergo a faster rate of cell death when subjected to either stronger deficit irrigation or elevated temperatures (Bonada et al., 2013ab). Likewise, Mendez et al. found that augmenting irrigation at 20 °Brix resulted in a greater berry weight (10%), while also suggesting an even greater need for irrigation in vines with greater crop load to prevent LSD-related loss—another study similarly demonstrates this strategy of ramping up irrigation post veraison (from 25% ET to 100%) resulting in increased berry weight by 13%

(Keller et al., 2016). Nevertheless, it would be prudent to determine the optimal timing and minimum threshold of post-veraison irrigation for postponing LSD considering the likelihood of increased water restrictions on growers in the future.

*Berry Hydraulics and Phenology*

Our current physiological understanding of berry hydraulics and ripening post-veraison explains why irrigation, and precise irrigation timing, could be critical to reducing late-season dehydration.

By the start of veraison, grape berries have completed the first segment of a double sigmoidal growth curve by the end of which cell division is complete and maximum berry size is fixed. This initial growth is due to the water potential in berry cells dropping as they accumulate solutes thereby drawing in water osmotically and increasing turgor pressure (Coombe 1980). It is not until veraison where berry elasticity and turgor pressure drop significantly before observed transcriptional changes occur to loosen cell walls for expansion—interestingly, it is not yet accounted for why turgor pressure drops prior to cell wall loosening (Castellarin et al., 2015). Berry turgor pressure continues to decline throughout ripening even as it achieves maximum volume.

After veraison, the last phase of berry cell expansion and growth is powered by sap transport into the berry through the phloem. The completion of veraison sees an important shift in the pathway of water transport into grape berries from the xylem to the phloem, reflecting a transition in phloem unloading from a symplastic to an apoplastic pathway that allows sugar to be unloaded

into the berry parenchyma cells against a concentration gradient. A proposed model by Keller et al. (2015) suggests that negative xylem water potentials from the canopy down to the berry exert a pulling force on water stored as sap in the parenchyma cells, drawing water through the apoplast into the xylem to be transpired in the canopy. Xylem backflow during ripening has been directly observed by Keller et al. (2006) and the relationship between xylem water potential, phloem unloading is evidenced by the observed increase in phloem flow into berries under drought stress (Keller et al., 2015). Similar to preparing a sauce reduction from simmering broth, grapevines start with a dilute sap unloaded by the phloem in the berry and leverage evapotranspiration in the canopy to concentrate sugars in the mesocarp. Thus, xylem backflow is a necessary to enable grapevines to reach sugar concentrations suitable for winemaking.

Once berries reach maximum size, usually at 24-25 °Brix, phloem transport and skin extensibility decline and further increases in sugar concentrations come from berry dehydration, either through xylem backflow or transpiration through the berry surface, though the latter declines steadily during ripening (Bonada et al., 2017; Matthews et al., 1987; Keller, 2010). Around this time, typically 90-100 days after anthesis depending on the variety, berries begin to lose weight and slowly shrivel. Mesocarp cell death, closely correlated with shrivel (Fuentes et al. 2010), begins near the seeds, eliminating what little turgor pressure is left and accelerating backflow through the xylem (Krasnow et al. 2008). Given that berry water potentials are not negative enough to slow down xylem backflow and phloem inflow is marginal, it is likely too late at this point for irrigation to effectively rehydrate berries. Alternatively, one way grapevines can reduce shrivel is to simply decrease hydraulic conductivity in the pedicel. Chardonnay has been shown to plug up xylem conduits in cane tissue with tyloses, which would reduce backflow

and therefore delay LSD, however it remains unclear whether this occurs in the pedicel and if other varieties demonstrate this tendency (Tilbrook and Tyerman 2009; Choat et al. 2009; Sun et al., 2008).

*Cell Death Mechanism*

There are at least two related metabolic pathways that occur at the onset of ripening that could contribute to the process of mesocarp cell death. For the first pathway, grape berries undergo a significant change in metabolism where malate is catabolized into pyruvate, which increases the respiratory quotient (i.e., the ratio of the amount of $CO_2$ produced to $O_2$ consumed) and diminishes the $O_2$ concentration in the berry to the point of hypoxia (Farmiani et al. 2013; Xiao et al., 2018b). Increasingly hypoxic conditions in the center of the mesocarp were correlated with greater cell death in Chardonnay and Syrah, with completely hypoxic conditions occurring at ~100 DAA, within the observed period of cell death in Syrah (Xiao et al., 2018a; Bonada et al. 2013a; Tilbrook and Tyerman 2008). This suggests that cultivar differences in onset and rates of cell death are in part due to variation in oxygen availability. Internal $O_2$ concentration is affected by the number of lenticels (pores) on the pedicel, which varies between varieties. For example, Xiao et al. (2018) found that the total surface area of lenticels on the pedicels was 10-fold larger in Chardonnay than Syrah, which could explain why Chardonnay exhibits slower rates of cell death (Bonada et al., 2013b; Tilbrook and Tyerman 2008). This process could also explain why higher nighttime as well as daytime temperatures accelerate cell death, since most berry respiration occurs at night (Bonada et al., 2013a). While seed respiration could to the post-veraison respiratory quotient shift. but respiration rates between seeded and seedless varieties do not significantly differ, suggesting that the vast majority of respiration occurs in the mesocarp

not the seeds (Xiao et al. 2018b). Seed respiration is significantly more active before veraison and declines once ripening commences (Harris et al., 1971).

A second pathway that is a main contributor to $CO_2$ production and malate degradation during ripening is ethanolic fermentation, which is needed to maintain cellular function as conditions become increasingly hypoxic (Terrier and Romieu, 2001). The increase in ethanolic fermentation increases the synthesis of alcohol dehydrogenase (ADH) to convert acetaldehyde to ethanol. This process generates hydrogen peroxide as an intermediate, which spurs negative feedback regulation of the attenuator of ROP-GTPase, thereby increasing ADH production (Fukao and Bailey-Serres 2004; Baxter-Burnell et al. 2002). This could account for how cell death persists and expands throughout the mesocarp.

Other research has posited that mesocarp cell death is not simply a consequence of normal berry metabolism, but another instantiation of the ubiquitous plant phenomenon of programmed cell death (PCD), the genetically regulated, physiological process of lysing unwanted cells via reactive oxygen species (ROS). In plants, ROS are metabolic by-products that serve as signals for biotic/abiotic stress responses and key phenological events. For example, stress from excessive light can cause singlet oxygen and hydrogen peroxide ($H_2O_2$) to accumulate in the reaction centers of the chloroplasts, though $H_2O_2$ typically plays a larger role in signaling for stress responses as the more stable intermediate (Triantaphylidès and Harvaux, 2009; Petrov and Van Breusegem, 2012; Mansoor et al., 2022). $H_2O_2$ also begins to accumulate at non-toxic levels in the skin at the onset of ripening for grapes and tomatoes, coinciding with transcriptional changes in ROS-regulating and oxidative stress-related genes (Pilati et al., 2007; Pilati et al.,

2014; Jimenez et al., 2002). The known role of ROS as signaling molecules (in plants generally) and the timing of its accumulation at veraison led Pilati to conclude that $H_2O_2$ is likely functioning as a signaling molecule at this time, though no direct evidence has been presented. Histone methyltransferases have been demonstrated to play regulatory roles in strawberry ripening (Gu et al. 2016) and their homolog in grapevines, *VvH3K4s*, was identified in table grapes by Liu et al. (2021) and shown to be regulated by $H_2O_2$. Only one study thus far has measured ROS and cell death in winegrapes, where Gowder (2022) found significant correlation between $H_2O_2$ and cell vitality in Syrah fruit in combined skin and mesocarp samples, still not indicating precisely enough whether *mesocarp* concentrations of ROS are connected to cell death. ROS damage in grape berries can be quantified indirectly through cell vitality staining and measured directly by the thiobarbituric acid assay which measures the lipid peroxidation product malondialdehyde (MDA) (Krasnow et al., 2008; Xi et al., 2017).

Despite the prevalence of ROS throughout major cellular components, plant cells prevent ROS from building up to toxic levels through ROS scavenging, using enzymatic (e.g. superoxide, peroxidase, catalase) and non-enzymatic (e.g. glutathione, ascorbic acid, phenolic compounds) mechanisms (Mansoor et al., 2022). However, the ROS scavenging capacity of grape berries becomes increasingly impaired over the course of ripening. Extractable tannins and procyanidins decrease sharply, largely due to the oxidation of phenolic compounds in the seed, which reduces ROS scavenging capacity right next to the area where mesocarp cell death begins (Ristic and Illand, 2005; Kennedy et al., 2000). Also, Shiraz berries have been reported to progressively decline in both their Ferric Reducing Antioxidant Potential and Diphenyl Picryl Hydrazyl Radical Scavenging ability (Shivashankara et al., 2013). However, the regulatory networks

regulating the scavenging and production of ROS are extremely complex and our understanding of specific mechanisms, including berry cell death, is limited.

Considering the extensive presence of PCD genes found in other plants, comparatively few have been identified in grapevines and none have been measured alongside an analysis of cell vitality dynamics. The first observations of PCD-related genes were reported by Pilati et al. (2007) who found that those associated with PCD suppression were downregulated and those associated with activation were upregulated between just before veraison and mid-ripening of Pinot Noir berries. Sweetman et al. (2012) published a transcriptome of Syrah that described an increase in the abundance of *VvBAP1* by an order of 7 from pre-veraison to full ripeness. Considering the proclivity of Syrah to shrivel, it may seem as though *VvBAP1* is a positive regulator of PCD, however Cao et al. (2019) further investigated this gene and found the opposite. Examining its expression in Syrah, the relative expression of *VvBAP1* was correlated with the degree of mesocarp cell death, and significantly downregulated at 92 DAA in a drought stress treatment, almost the exact time of cell death onset found by Bonada et al. (2013b). This negative regulation of PCD was further confirmed in other organisms: its expression in Arabidopsis, tobacco, and yeast significantly improved tolerance to $H_2O_2$, resulting in plant tissue and cells with less oxidative damage. It was previously mentioned that $H_2O_2$ can act as a benign signal at low concentrations, however it has also been observed to function as a trigger for programmed cell death via a signal transduction pathway (Levine et al., 1994; Neill et al., 2002).

The typical parameters used to monitor the ripening of commercial wine grapes are acid catabolism (declining TA/increasing pH), sugar accumulation, the accumulation of phenolic

compounds, seed maturity, and flavor development. As was previously shown, the latter two are physiologically and sensorily implicated in the onset of mesocarp cell death and late season dehydration. Delaying the onset of cell death would enable winemakers to continue the practice of extended hangtime for desired wine characteristics while preventing unwanted yield losses for growers. When during ripening is the optimal time to relieve water stress and how much relief is needed in the form of irrigation volume has yet to be elucidated. A more nuanced picture of the timing and bare minimum amount of irrigation needed will prepare growers for a likely future under water restrictions.

As a first measure, we set out to investigate whether additional pulses of irrigation prior to or during the onset of cell death in Cabernet Sauvignon berries would either postpone onset or delay the rate of cell death. We hypothesized that an early pulse two-weeks prior to projected cell death onset would relieve water stress and hold over triggers for programmed cell death. A later pulse of irrigation concurrent with projected cell death onset was expected to insufficiently compensate for accelerated xylem backflow at a time of diminishing phloem inflow. We addressed the need to connect ROS in the mesocarp to cell death by measuring $H_2O_2$ and MDA concentrations in skinned and seeded grape samples, anticipating that their accumulation would coincide and track with the progression of mesocarp cell death.

## Materials and Methods

*Plant Material and Irrigation Treatments*

This study used mature Cabernet Sauvignon grapevines planted on 420A rootstock growing in an experimental vineyard on the University of California, Davis campus in Davis, CA. Vines were cane pruned and trained to a VSP system planted 7 feet apart with 11 feet between rows. Canopy and pest management followed standard commercial practices. Anthesis occurred on May 15$^{th}$ 2022 and veraison, defined by 50% of the clusters with at least one colored berry, occurred at approximately 58 days after anthesis (DAA).

Vines from one row were randomly assigned to either a control, early, or late irrigation treatment ($N$ = 5 vines/treatment). Vines from different treatments were separated by two buffer vines, each subjected to the same irrigation regime as the adjacent experimental vine. The control treatment used a standard regulated deficit irrigation regime for a hot growing region. Prior to the experimental period, vines were irrigated weekly starting one month before anthesis at 35% replacement of evapotranspiration (RDI), which was estimated using a crop coefficient-based $ET_c$, vineyard spacing, and precipitation as parameters. One month after bloom and through veraison, RDI was increased to 50% and further increased to 70% in anticipation of forecasted heatwaves. Irrigation frequency was increased to every 2 – 3 days during the experimental period (July 25 to August 26, 2022), to ensure the treatments had enough time to affect soil moisture in the root zones. Control vines received 0.45in for the first week of the experimental period, then 0.34in for the rest of the period (Fig. 1). Vines in the early and late treatments received the same irrigation as the control, except for an additional 'pulse' that increased irrigation to 0.54in/week for two weeks. The early treatment 'pulse' was applied in the two weeks before the expected

onset of cell death (July 25 to August 5) and the late treatment ‘pulse’ was applied in the two weeks after (August 8 to August 22). The projected cell death onset for our study was based on the only other study tracking phenology and cell death (due to late-season dehydration) of specifically Cabernet Sauvignon fruit (Krasnow et al. 2008).

During the first week of the first irrigation treatment pulse a 20% difference in irrigation volume was applied to the vines, with the early vines received 0.56 in while the late and control treatments received 0.45 in. After seeing little remediation of water stress by the end of the first week, that difference was increased to 40% the second week by reducing the water applied to the late and control vines to 0.34 in (Figure 1). This difference was maintained for the late irrigation pulse, yet in the final week of sampling the weekly volume was reduced to .22 in.

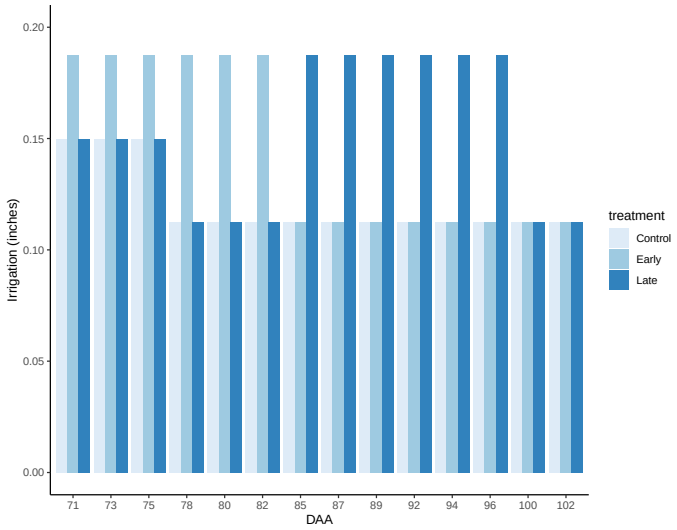


**Figure 1** Irrigation volumes over the experimental period. Vines were watered 3x/week except for the final week (100-102 DAA) they were watered twice.

*Gas Exchange and Water Potential*

Vines were monitored for water stress by measuring gas exchange and midday stem and pre-dawn water potentials weekly over the experimental period. Pre-dawn leaves were sampled from $0400_{HR}$ to $0500_{HR}$ and placed in a humidified bag immediately after excision from the shoot ($N$ = 2 leaves/vine). Midday leaves were sampled and measured for gas exchange from 1200 to $1330_{HR}$ and were covered in a humidified, foil-wrapped bag for 20 minutes before excision to equilibrate water potential in the stem and the leaf ($N$ = 30 leaves). Leaf selection was limited to sun-exposed, mature leaves at a distance of 8-12 leaves from the shoot tip. Bagged leaves were immediately placed in a cooler after excision, then transported to the lab and measured for water potential with a pressure bomb within one hour of sampling. Photosynthesis (A) and stomatal conductance ($g_s$) were measured weekly at the same time and in the same manner as midday water potential sampling using a LICOR 6800 gas exchange system.

*Berry Sampling*

Four clusters per vine were marked for repeated sampling ($N$ = 20 clusters/treatment). 1 berry/cluster was sampled each for FDA staining and ROS analyses on 9 dates over the experimental period ($N$ = 20 berries/treatment). 1 berry/cluster was sampled for transcriptomics on 3 dates before and after the expected onset of cell death (August 3, 10, and 22). Size, color, and softness were used to select berries that were relatively advanced in maturity. Berries were excised with the pedicel attached and transported on ice to the laboratory. Sampling continued until total soluble solids (TSS) reached 27 °Brix, at which point the rest of the cluster was crushed, and the grape must analyzed for TSS, titratable acidity (TA), and pH.

*Cell Vitality Staining*

The FDA staining technique from Krasnow et al. (2008) was used to quantify berry cell vitality. First, we made a transverse cut with a razor blade to remove 1-2 mm from the pedicel end of the berry, to locate the seeds. We then cut the berry in half longitudinally between the seeds, keeping the blade as close to the center of the berry as possible. One half of each berry was then placed in a humidified petri dish and refrigerated and the other half was crushed and the juices homogenized with the other berries from the same vine. Juice samples were measured for osmotic potential with a Vapro 5600 vapor pressure osmometer. The refrigerated halves were stained with a 9.6 uM FDA solution prepared by adding 2ul of 4.8mM FDA stock solution (in acetone) to 1ml of sucrose solution with the same osmotic potential as the juice samples, to avoid cell death from osmotic shock. Preliminary trials by Krasnow et al. (2008) showed that variability in osmotic potential between berries from the same vine was small and that using homogenized samples did not make differences between solutions and berry osmotic potentials larger than 0.5 MPa thresholds are recommended to avoid osmotic shock. Berry halves were blotted with a kimwipe dipped in the staining solution to remove cellular debris and sectioned again to obtain a 2-3 mm thick longitudinal cross section without seeds. Sections were then abundantly coated in the staining solution and allowed to take up the solution for 30 minutes before imaging.

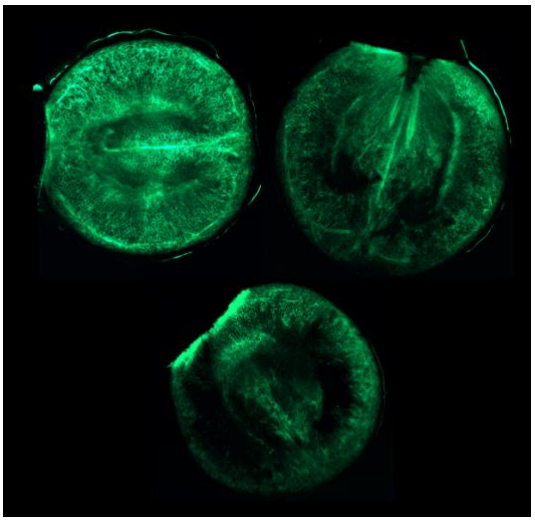

**Figure 2a** Fluorescein Diacetate-stained berries at progressive stages of cell death originating deep in the mesocarp tissue near the seeds.

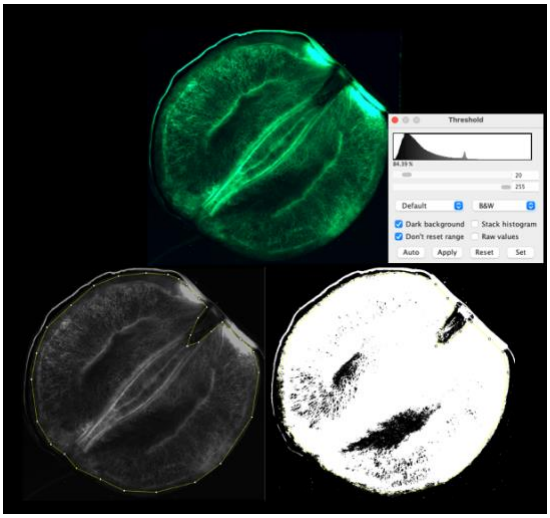


**Figure 2b** A berry image in color, grayscale, then finally subjected to a pixel-intensity threshold. Berries measured for perimeter and area measurements were traced differently, not omitting the pedicel area, as shown above, to accurately measure perimeter.

*Microscopy*

Stained berry sections were visualized with fluorescent microscopy (Figure 2a) using a Leica DM4000B microscope equipped with a Leica DFC 320 camera and Leica GFP filter cube. The camera was operated with Leica Application Suite Software (version 7.4). Camera settings, including gamma, exposure, gain, and contrast, were held constant for all images. Each berry was photographed at 1.4x magnification in four images that were stitched together with Adobe Photoshop (version 23.5.3).

*Cell Vitality and Berry Shrivel Analyses*

Percent cell vitality and berry perimeter (P) and area (A) were measured with ImageJ software (NIH). Berry perimeters were traced by hand on the stitched images before the image was converted to grayscale, then a pixel intensity threshold was chosen to accurately capture the proportion of living tissue in the original image (Figure 2b). Thresholds were typically set just

after the first peak (thresholds descending) in the Set Threshold function. Removing noise did not significantly alter either measurement.

Perimeter and area were then used to calculate the Berry Shrivel Index from Fuentes et al (2010):

$$R = \frac{A}{P}$$

$$ShI = \frac{R - R_{min}}{R_{max} - R_{min}}$$

where R is the A/P ratio for an individual berry and $R_{max}$ and $R_{min}$ are the maximum and minimum ratios across the entire dataset. Berry Shrivel Index ranges from 0-1, with 0 representing a completely shriveled berry, and 1 a fully turgid berry.

*Hydrogen Peroxide/Malondialdehyde Analysis*

Berries sampled for ROS and lipid oxidation products (MDA) were immediately frozen in liquid nitrogen and stored in a -80°F freezer. The mesocarp tissue was isolated by peeling the frozen berries with a scalpel, then gently breaking and deseeding the frozen pulp. The four berries sampled per vine were then homogenized and ground to a fine powder in liquid nitrogen ($N$ = 5 vines/treatment). $H_2O_2$ concentrations were measured with an Amplex®Red Hydrogen Peroxide/Peroxidase Assay kit, following Pilati et al. (2007). This is a fluorimetric assay quantifying the absorbance of 10-acetyl-3,7-dihydroxyphenoxazine, which fluoresces red when oxidized in the presence of $H_2O_2$ and peroxidase. 0.2g of powder was solubilized in 0.5ml of 50mM phosphate buffer (pH 7.4) and kept on ice for 5 minutes. The mixture was centrifuged at 20,000 g for 15 minutes, after which 0.4 ml of supernatant was extracted, mixed with 0.4 ml of 2:1 (v/v) chloroform:methanol mixture, and centrifuged at 12,000 g for 5 minutes. 50ul of

supernatant was combined with 50ul of Amplex®Red working solution, which was prepared according to manufacturer instructions, in a black 96-well plate with a transparent flat bottom. Absorbance was read using an Epoch-2 microplate reader at 560nm. For $H_2O_2$ quantification, a standard curve was generated following the manufacturer's instructions.

The method of Sun et al. (2011) was followed to measure MDA content for grape berries. Frozen grape powder (0.25g) was homogenized for 10min in 0.1% (w/v) trichloroacetic acid and then centrifuged at 10,000 g for 5 minutes. 1mL of the supernatant was combined with 4mL 20% (w/v) trichloroacetic acid containing 0.5% (w/v) thiobarbituric acid, then the mixture was heated for 15 minutes at 95°C then immediately cooled in an ice bath for 5 minutes. After centrifugation at 10,000g for 10 minutes, $100\mu L$ of supernatant was plated into a Corning® black-walled, clear, flat-bottomed 96-well plate and absorbance were read at 532 and 600 nm. Concentration was calculated using the MDA molar extinction coefficient 155,000 $M^{-1}cm^{-1}$ with the following equation: MDA concentration (nmol/g FW) = $(A_{532\text{-}600}/155{,}000)\bullet 10^{10}$, accounting for aliquot volumes and dilution factors.

*Statistical Analysis*

The effect of the irrigation treatments on indicators of vine water stress, hydrogen peroxide/lipid oxidation products, and osmotic potential in the berry was examined through one-way analysis of variance for each sample date.

We determined the onset and rate of berry cell death, shrivel, and ROS accumulation by fitting piecewise linear regression models (using the 'segmented' package in R, version 4.3.1) between

time and percent cell vitality, the berry shrivel index, and $H_2O_2$ concentrations. The onset is the date these variables transitioned from relatively constant to rapidly changing, defined as the fitted breakpoints of the piecewise regression models, and the rate is the slope of these variables over time after onset. We tested for significant irrigation treatment effects on onset and rate by examining their 95% confidence intervals for overlap. Furthermore, Correlation between shrivel and % living tissue and peroxide and % living tissue was determined through the Standardized Major Axis Tests and Routines (SMATR) package in R using the sma function.

We also tested for significant treatment differences between treatments by one-way analysis of variance for TSS, TA, and pH at harvest, when they are most relevant to growers.

Because 7/25 was not used for perimeter analysis, nor was 8/1 for cell vitality, both sets of data were omitted in order to achieve a date-by-date correlation. Out of 540 berries sampled, 248 cross sections were viable for image analysis due to damage incurred in the mesocarp from the razor blade hitting and dislodging seeds. Measurements of percent living tissue and perimeter/total area were taken on different yet mostly overlapping subsets of images due to a fraction (32%) of images lacking a smooth perimeter or consistent dye stain. For cell vitality analysis, n = 68, 65, and 72 for treatments 1, 2, and 3 respectively; and for the shrivel index analysis, n = 74, 65, and 78 for treatments 1, 2, and 3 respectively. In tracing representative areas of the berry for cell vitality analysis, the selected area routinely excluded the pedicel residue, which did not typically take up the stain. Due to the violations of equal variance caused by these asymmetries, the non-parametric One-Way test in R was used for both percent living tissue and

shrivel index on the last sampling date, and, likewise, the Games-Howell test was used as a post-hoc test to compare treatment groups.

## Results

*Water Stress Indicators*

Midday and pre-dawn stem water potentials ($\psi_{md}$ and $\psi_{pd}$) were similar between treatments, and typical for commercially-grown winegrapes (Girona et al., 2006) in the late ripening period between veraison and harvest (Table 1). Treatment means for $\psi_{pd}$ ranged from -0.34 to -0.61 MPa and for $\psi_{md}$ ranged from -1.07 to -1.45 MPa over the experimental period (Table 1). $\psi_{md}$ generally increased during the experimental period, ranging from -1.19 to -1.71 on the first sampling date and from -0.77 and -1.40 MPa on the last, while there was little change in $\psi_{pd}$ (Figure 3). The early and late augmented irrigation treatments did not cause significant differences in $\psi_{md}$ or $\psi_{pd}$ for all sampling dates ($p > .05$).

The irrigation treatments also did not produce significant differences in gas exchange. Treatment means ranged from 11.4 to 16.7 μmol $m^{-2}$ $s^{-1}$ for photosynthesis (A) and from 0.18 to 0.27 mol $m^{-2}$ $s^{-1}$ for stomatal conductance ($g_s$) over the study period (Table 2). Photosynthesis and stomatal conductance were only significantly different between treatments during the early irrigation 'pulse', but, contrary to expectation, were only significantly higher for the late treatment vines, which were not receiving additional irrigation on these dates (Figures 4,5). Gas exchange rates decreased and converged between treatments over the experimental period, and gas exchange was not significantly different between treatments on any other sampling dates.

*Onset and Rate of Cell Death*

Our augmented irrigation regimen commencing on the estimated date of onset, i.e. the late treatment, was effective in significantly reducing the rate but not the onset of cell death. Onset was defined as the fitted breakpoint of the piecewise linear regression (PLR) models, when the rate of change in cell vitality significantly increased. The onset of cell death occurred 92 ± 1 (mean ± standard error) DAA for the control, 89 ± 8 DAA for the early treatment, and 83 ± 4 DAA for the late treatment (Table 3). The 95% confidence intervals for these estimates overlapped, indicating that onset was not significantly different between treatments. The fitted slope after the breakpoint indicates the rate of cell death after onset. Post-onset slopes were -2.06 ± 0.22 for the control, -1.21 ± 0.53 for the early treatment, and -0.90 ± 0.11 for the late treatment (Table 3). The significance of the late treatment's effect on the rate of cell death is demonstrated by the non-overlapping 95% confidence intervals between the control and late treatment. There were no final treatment differences found on cell vitality for the last sampling date. Figure 6 displays the cell vitality means (± se) while Figure 7 shows the segmented fit over the means.

*Shrivel Index*

At harvest, the late treatment was determined to be significantly less shriveled than the early treatment. Contrary to the expectation that berry turgidity and the shrivel index would continually decline over the ripening period, tracking the decline in cell vitality, the shrivel index fluctuated over time (Figure 8). By PLR analysis, the breakpoint of the control was 89 DAA with initial/final slopes m = 0.007 and m'= -0.021, while the early and late treatments respectively were 74 DAA with slopes m = 0.02 m'= -0.011, and 79 DAA with slopes m = 0.001 and m'= -0.014 (Table 3). We did not find significant correlation overall between cell death and shrivel (p

> 0.05) through our SMATR analysis (Figure 11), however only for the control treatment was significant correlation found ($p < .05$).

*Hydrogen Peroxide and MDA*

Approximately concurrent with the onset of cell death, $H_2O_2$ began an upward trend at 85 DAA (Figure 9) and significantly correlated with cell vitality (Figure 12). Peroxide content was initially ~1.7 nmol/gFW, and generally increased to ~3nmol/gFW. One-way analysis of variance revealed no treatment effects for all dates, nor did a PLR model reveal a similar breakpoint to observed cell death. SMATR analysis revealed a significant correlation between $H_2O_2$ and cell death for the late treatment and control ($p < .05$).

MDA on the other hand did not persistently accumulate in the mesocarp but in general fluctuated throughout ripening (Figure 10). Mean concentration at 71 DAA was ~1.4 nmol/g FW, approximately the same as at 96 DAA yet slightly increased later at 99 DAA to ~1.5 nmol/g FW. Two-way ANOVA yielded no significant treatment differences in MDA concentration for any of the dates.

*Osmotic potential*

Osmotic potentials were not found to be significantly different between treatments by one-way ANOVA for all sample dates. Osmotic potential measurements were used for creating FDA solutions and tracking berry maturity (Figure 13), as osmotic potential is directly correlated with soluble solids in the berry. Figure 14 displays Brix values obtained from our osmotic potential measurements using a linear equation from Bondada et al. (2017) modeling Merlot grapes.

*Fruit Quality At Harvest*

Remaining fruit on the last day of sampling was harvested and pressed by hand into composite vine samples. Final Brix values observed were in the target range, ~27, mimicking typical ranges of those found in wineries producing Cabernet Sauvignon wines from a warm climate. Juice analysis revealed no significant differences in Brix, pH and TA, as shown in Table 4.

## Discussion

*Cell Death and Shrivel*

Our late irrigation treatment, a 40% augmented pulse starting at the beginning of cell death, generated two significant effects in our experiment: it reduced the rate of cell death in the berry mesocarp tissue and produced less shriveled, more turgid berries at harvest. We also hypothesized that the early treatment would preemptively reduce water stress and postpone cell death. We correctly anticipated the date of cell death onset (~90 DAA), yet despite the optimal timing of our treatments the early irrigation regime was not successful in reducing water stress or cell death. While the late pulse reduced the rate of cell death, its effect on shrivel at harvest was not present for the rest of the experiment. This asymmetry is highlighted by the lack of overall correlation between shrivel and cell death for the late pulse, and the lack of a steady decline in turgidity (Figure 6). It was only for the control that significant correlation was observed, which may be explained by the lower error observed in the piecewise linear regression model for the control than the late or early treatments (Table 3). Unexpectedly, the greater turgidity in the late treatment berries was not reflected in the osmotic potential, °Brix, or TA measurements at

harvest, when we would have expected solutes to be more dilute than treatments with greater shrivel (Table 4). While significant, difference in shrivel were not great enough to affect solute concentrations.

The cell death onset and rates we found were largely within the range observed in other studies, but it can be difficult to draw definitive conclusions from comparing the onset and rate of cell death among experiments with many changing variables (e.g. irrigation design, volume and timing of additional rainfall, growing degree days, rootstock, cultivar, and calendar units). Cabernet Sauvignon has only been measured in one other study (Krasnow et al., 2008) with cell death beginning at 100 DAA and 40 days after veraison (DAV) for field-grown vines in Napa Valley (Oakville), compared to 92 DAA and 34 DAV for our control vines in Davis (Figure 6). Given Davis is a warmer climate than Oakville, this may explain why our vines exhibited cell death onset earlier. These differences could also reflect a lack of precision in estimating onset dates, since fluctuations in %living tissue measurements can weaken trends with time, as in this study (Figure 6). This could also reflect differences in growing conditions or typical variation within cultivars. The reported ranges of cell death onset dates for any given cultivar vary by as much as 12 days. Syrah (Shiraz) onset tends to fall between 87-96 DAA after which tissue vitality sharply declines (Bonada et al., 2013b; Xiao et al., 2018; Gowder 2022) while Chardonnay's cell death much slower at an approximately constant rate. (Krasnow et al., 2008; Bonada et al., 2013b).

Our rates of cell death (Table 3) fell within the reported range of living tissue analysis performed thus far on grape berries. The Cabernet in Krasnow et al. (2008), between 100-150DAA, lost cell

vitality at a rate of approximately -0.83 %LT/DAA while our control and early treatments for Cabernet had a rate of -1.21 and -2.06 respectively. Metabolic processes sensitive to temperature have been connected to cell death, however Xiao et al. (2018) and Bonada et al. (2013b) have both observed no impact of elevated temperature on cell death rate. For Bonada et al. (2013b), within the range of 80-120DAA, Syrah lost living tissue at a rate of -0.62 %LT/DAA and Chardonnay at -0.53. The greatest rate of cell death was reported by Xiao et al (2018) with living tissue in Syrah diminishing at rates as high as -5.17 %LT/DAA. Interestingly, Xiao et al. found that irrigation postponed cell death onset much later than the non-irrigated vines, yet the irrigated vines crashed twice as fast (-5.17 %LT/DAA) as the non-irrigated vines (-2.35 %LT/DAA), which may have developed more extensive root systems with greater access to water. Conversely, our late treatment vines exhibited the slowest cell death and the earliest onset, highlighting the efficacy in slowing cell death.

Our results for cell vitality and shrivel analysis accord with the reported role that xylem backflow plays in the relationship between cell death and LSD. Cell death occurs prior to LSD by reducing turgor pressure and accelerating water loss through xylem backflow, thus a more negative $\psi_x$ would enhance the pulling force for water out of the berry (Keller et al., 2015). Since $\psi_{md}$ and berry osmotic potentials were nearly the same across treatments, the observed differences in cell death rate and shrivel index cannot be attributed to differences in xylem water potential ($\psi_x$) or the berry solute concentrations. In the late treatment berries cell death was slower and cell vitality remained greater (Figure 6) from 92DAA onwards (though not significantly), which indicates more water retention and less backflow. Less water loss in berries from cell death supports our finding that the late treatment berries maintained the greatest

turgidity for almost all dates during that same period, from 92DAA to harvest. Another factor to consider affecting xylem backflow is pedicel hydraulic conductivity. Xylem blockages (polysaccharides) that are known to develop post-veraison in grapevines could hinder pedicel hydraulic conductivity and slow down backflow out of the berry (Knipfer et al., 2015), though there is no basis for such a physiological response to our late irrigation pulse. There are established differences in pedicel hydraulic conductivity between grape cultivars post-veraison and it has been reported that grapevines produce tylose blockages in response to pruning wounds and bacterial infection (Tilbrook and Tyerman 2009; Tilbrook and Tyerman 2004; Sun et al., 2008; Sun et al., 2013). Yet, there is no reported evidence of grapevines producing xylem gel-blockages in relation to water stress during our period of ripening.

For future studies, it may be of interest to track phloem inflow to the berries in response to extra water availability during cell death. Post-veraison the phloem remains the main source of water influx into the berry, remaining functional until 25-26 Brix, a range our berries did not exceed during the late treatment pulse, which suggests the phloem likely remained functional (Bonada et al., 2017; Keller 2010). Our results have shown vines receiving additional irrigation during the onset of cell death, despite having an earlier onset of cell death, retained water better than vines with later onset. Since phloem functionality declines steadily during ripening (Evert, 1982), an earlier onset of cell death comes at a time of potentially greater phloem hydraulic conductivity, rendering an irrigation pulse more effective at providing more phloem inflow to compensate for xylem backflow. Greater sap influx into the berry would introduce more dissolved oxygen and alleviate hypoxic stress due to respiration and ethanolic fermentation, though this has not been experimentally determined.

*ROS and MDA*

We expected that $H_2O_2$ levels to begin to rise at cell death and continue throughout the experiment. Our $H_2O_2$ concentrations saw an uptick during the onset of cell death and, with exception of one outlying date, steadily increased throughout cell death proliferation at similar levels for all treatments (Figure 9). Across the three treatments cell death onset (85-90 DAA) coincided with the onset of $H_2O_2$ accumulation at 88 DAA (Figure 6; Figure 9). This is evidenced by the significant correlation found between the two variables for the late treatment and the control. It should be noted that it is only coincidental that those same two treatment groups were significantly different in our cell death rate analysis—matching significant $H_2O_2$ correlations and cell death rates would not be causally related findings. Whether the concentrations found in our study, between 1-3 nmol/g FW, are great enough to cause the degree of cell death we observed is not clear. Gowder (2022) measured $H_2O_2$ in combined skin and pulp samples finding concentrations in the range of 4-10 nmol/gFW in Chardonnay, 12-9 in Grenache, and 15-40 nmol/gFW in Syrah between 90-120 DAA with similar percentages of living mesocarp tissue to this experiment. We would expect to find lower values in the mesocarp only given that the skin is known to contain higher levels of $H_2O_2$, yet Pilati et al. (2014) found values in range of 18-27 nmol/gFW for the mesocarp only of Pinot Noir berries between 70-84 DAA. Interestingly, also in Gowder (2022) the three cultivars expressed no clear relationships between $H_2O_2$ accumulation and cell death, indicating there is much greater complexity to be addressed in the sources of $H_2O_2$, its scavenging, and alternative causes of cell death such as lipoxygenases. That there are wide cultivar differences in these relationships leaves open the possibility our chosen cultivar, Cabernet Sauvignon, has naturally low concentrations.

Despite the expectation that the products of membrane lysis would track with its causative reactive oxygen species, MDA concentrations did not commence at cell death onset or follow $H_2O_2$ concentrations and similarly saw no differences caused by either irrigation pulses. Like $H_2O_2$, MDA is a signal and damaging reactive compound subject to regulatory networks addressing biotic and abiotic stress, thus, accounting for its presence is not straightforward. In its most reactive state (pH < 4.46) and at high levels, MDA can damage proteins, nucleic acids, and photosynthesis-related proteins, while at lower levels it can serve as a signal activating (like $H_2O_2$) alcohol dehydrogenase (ADH). This activation helps achieve redox homeostasis by producing NADPH, which in turn oxidizes aldehydic compounds like MDA to prevent their build up to toxic levels (Tagnon and Simeon, 2017; Zhao et al., 2018). Post veraison, cellular conditions continue to be more favorable for the proliferation of ROS as scavenging and antioxidant capacity diminishes, whereas MDA may be more favored for degradation as ADH is more active then due to increased ethanolic fermentation in hypoxic conditions. Considering these processes we would have expected our MDA values to spike during cell death and then decline as hypoxic conditions maintained, but they ended the experiment at roughly the initial levels (Figure 10).

*Efficacy of Irrigation Treatments*

Our experiment attempted to establish significant differences in water stress before and during cell death onset to test whether late-season-dehydration-related processes respond to irrigation pulses at those timepoints. Despite a 40% increase in volume in subsequent two-week periods, vines under different irrigation regimes showed no treatment effects across all water stress parameters. The only difference was that the late pulse vines began the experiment with

significantly higher stomatal conductance and photosynthesis rates (Figure 4ab), yet by the time the late pulse occurred these differences were erased.

Other experiments investigating the relationship between water stress and cell death maintained consistent differences in watering throughout the growing season and found significant effects on both $\psi_{md}$ and cell death dynamics (Bonada et al., 2013b, Xiao et al., 2018). We sought a strategy fit for implementing late in the season when root systems and canopies are fixed, and irrigation treatments would only affect post-veraison processes related to cell death. Root growth after veraison is largely inactive as the vine expends more energy into reproductive growth, thus our water treatments would not have spurred much new root growth but rather provided more water availability to fixed root systems. This water would be largely available because of the sizable portion of clay in our soils, though soil moisture probes would be needed to confirm the late treatment had significantly more water available. The low-vigor rootstock used in this study, 420A, could have limited the efficacy of our treatments due to its lower root hydraulic conductivity and aquaporin activity, whereas high-vigor, drought-avoidant rootstocks such as 140Ru, could have rendered the treatments more effective (Gambetta et al., 2012). For example, after irrigating minimally pre-veraison, Netzer et al. (2019) imposed an augmented irrigation regime of .55in/week during a 45 day period post veraison for Cabernet Sauvignon on 140Ru in a Mediterranean climate with sandy soils and found continuously improving $\psi_{md}$. A higher-vigor rootstock could have enabled our vines to transpire all of the water that was available to them, reduce $\psi_{md}$, potentially prompting a different response. Given Netzer et al.'s success with alleviating water stress in late ripening, to achieve clarity on the effectiveness of late season

irrigation pulses on water stress and cell death, it may be advantageous to use a high vigor rootstock under stronger drought conditions pre-veraison before irrigation is augmented.

Of additional consideration regarding the similarity of $\psi_{md}$ across our treatments is that the vines used in this study were pruned by students, not an experienced crew, which does not guarantee uniformity in sap flow or canopy environment. Pruning without respect to sap flow—that is, year-after-year pruning cuts are made adjacent to each other to minimize the redirection of sap flow—has been shown to effect negative changes in xylem hydraulic conductivity in grapevines (Claverie et al., 2023). The strong relationship found between xylem hydraulic conductivity and photosynthetic capacity of the canopy indicates this would have also affected our gas exchange measurements (Brodribb, 2009). Without a consistent approach to pruning among our vines in this respect, variance in xylem hydraulic conductivity could have created enough statistical noise to mute differences in gas exchange and water potential.

*Conclusion*

This study demonstrated that increasing irrigation at the onset of cell death in winegrapes can delay the rate of cell death and maintain greater membrane integrity. When cell death is reduced, xylem backflow, which is difficult to compensate for as cell death progresses, is held off and turgidity is better preserved. Our results also confirm both the approximate range of onset date for Cabernet Sauvignon and the direct relationship between reactive oxygen species and cell death. The exact mechanism of cell death remains opaque and many questions remain as to how cell death ought to be managed, especially in drought conditions. It is ultimately unclear why the late treatment's cell death rate was positively affected by the late pulse, as we would expect

xylem backflow to be too strong to overcome once cell lysis proliferates, considering there was no difference in water stress across treatments. Nonetheless, we believe this opens the door to more paths of inquiry in the mechanism of cell death. To investigate why a pulse of irrigation near cell death can effectively delay cell death without altering gas exchange or stem water potentials will require monitoring additional parameters, such as xylem/phloem conductivity in the pedicel or peduncle, dissolved oxygen ingress into the berry, berry respiration/fermentation rate, and soil moisture. On the other hand, establishing firm differences in water stress prior to onset would clarify whether the activity of programmed-cell-death-related genes does in fact respond to increased water stress and account for increased ROS and cell death. Establishing such differences would also clarify how far in advance a preemptive transcriptional response occurs, which would inform the timing of proposed irrigation strategies to postpone or delay cell death onset. A framework for an efficient irrigation regime that postpones cell death onset is needed to address future water scarcity, and our treatments and the levels of irrigation applied throughout this experiment are far from optimal to this end.

## Figures

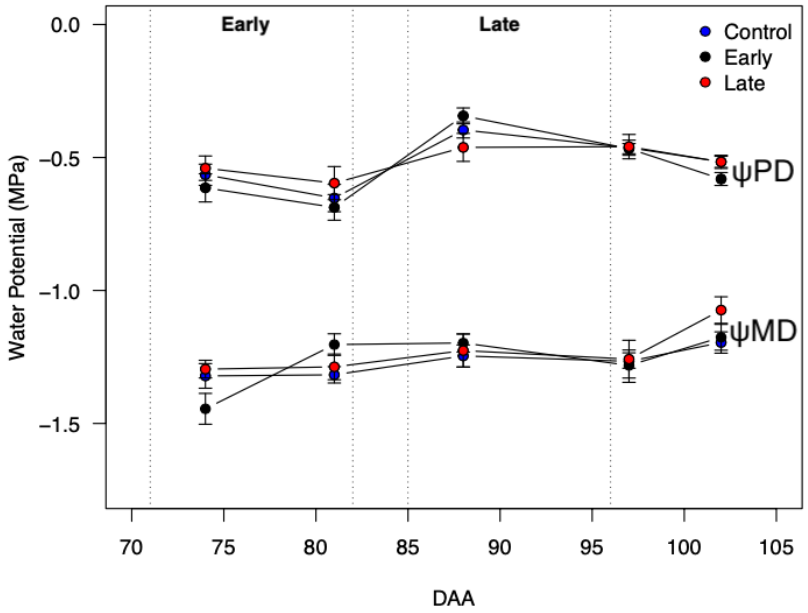


**Figure 3** Midday and Predawn weekly water potentials, error bars indicate standard error, n= 30. For each date, One-Way ANOVA determined p>0.05. Vertical dashed lines indicate treatment periods. The early treatment spanned 71-82DAA and the late treatment spanned 85-96DAA.

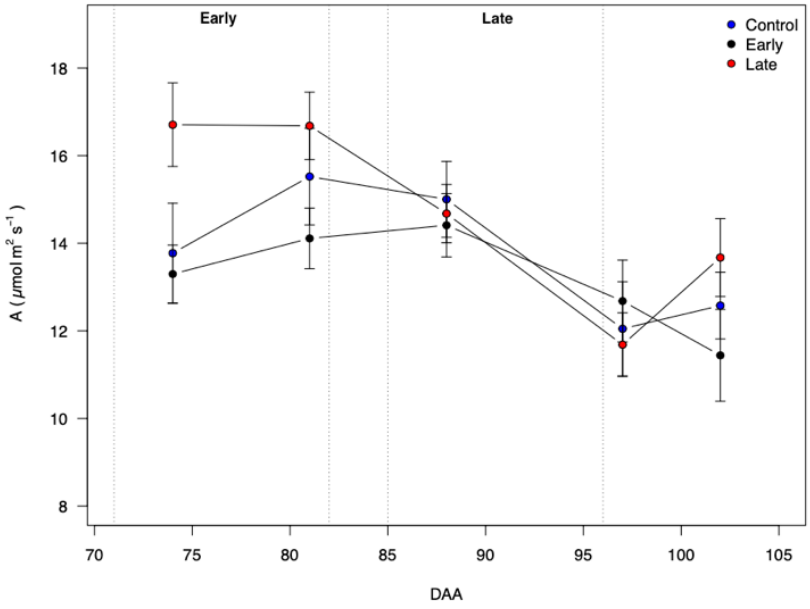


**Figure 4** Comparison of net photosynthetic $CO_2$ assimilation rate ± standard error, n = 30. At 74DAA date, One-Way ANOVA and Tukey's HSD test determined p<0.05, with the late treatment significantly larger than the control. For all other dates p>0.05. Vertical dashed lines indicate treatment periods. The early treatment spanned 71-82DAA and the late treatment spanned 85-96DAA.

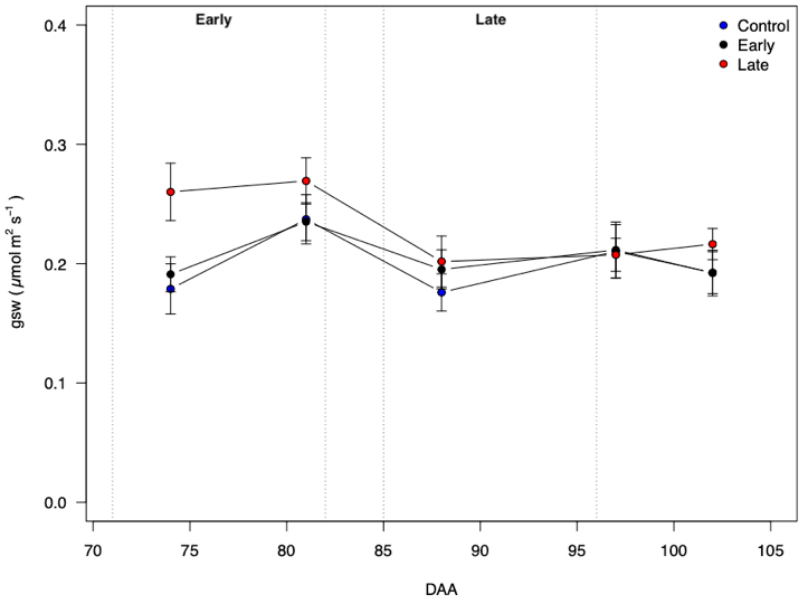


**Figure 5** Comparison of stomatal conductance rates ± standard error between treatments, n = 30. At 74DAA date, One-Way ANOVA and Tukey's HSD test determined $p<0.05$, with the late treatment significantly larger than the control. For all other dates $p>0.05$. Vertical dashed lines indicate treatment periods. The early treatment spanned 71-82DAA and the late treatment spanned 85-96DAA.

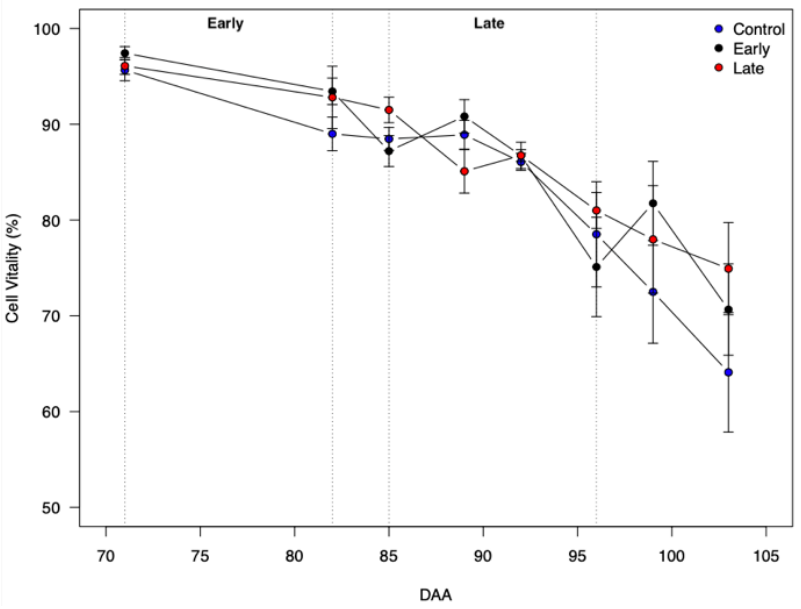


**Figure 6** Dynamics of cell vitality means ± standard error during the experimental period. Sample size slightly varied by treatment: control n = 68, early pulse n = 65, late pulse n = 72. Vertical dashed lines indicate treatment periods. The early treatment spanned 71-82DAA and the late treatment spanned 85-96DAA.

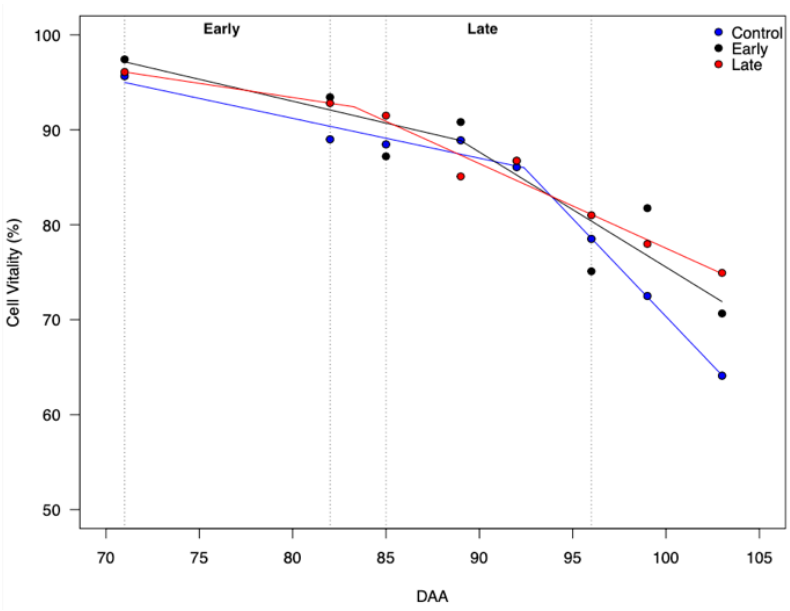


**Figure 7** Piecewise linear regression model of cell death onset and rate. Breakpoints signify where the two linear models for each treatment group are joined, in our case this indicates the approximate onset of cell death. 95% confidence intervals for post onset slopes indicated the late treatment was significantly slower than the control. Vertical dashed lines indicate treatment periods. The early treatment spanned 71-82DAA and the late treatment spanned 85-96DAA.

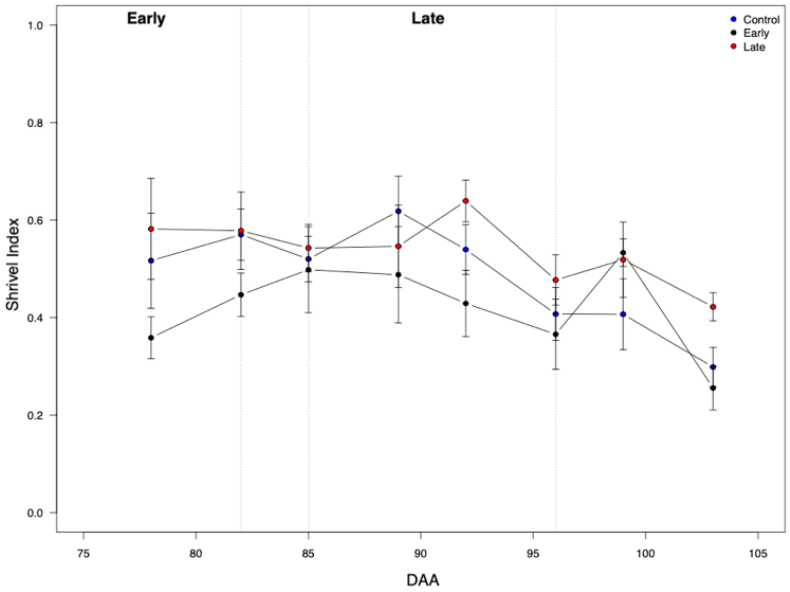


**Figure 8** Shrivel Index means ± standard error. Larger index values indicate a more turgid berry relative to the whole data set. Sample size slightly varied by treatment: control n = 74, early pulse n = 65, late pulse n = 78. One-Way Test determined $p<0.05$ at 103DAA and for all other dates $p>0.05$. Vertical dashed lines indicate treatment periods. The early treatment spanned 71-82DAA and the late treatment spanned 85-96DAA.

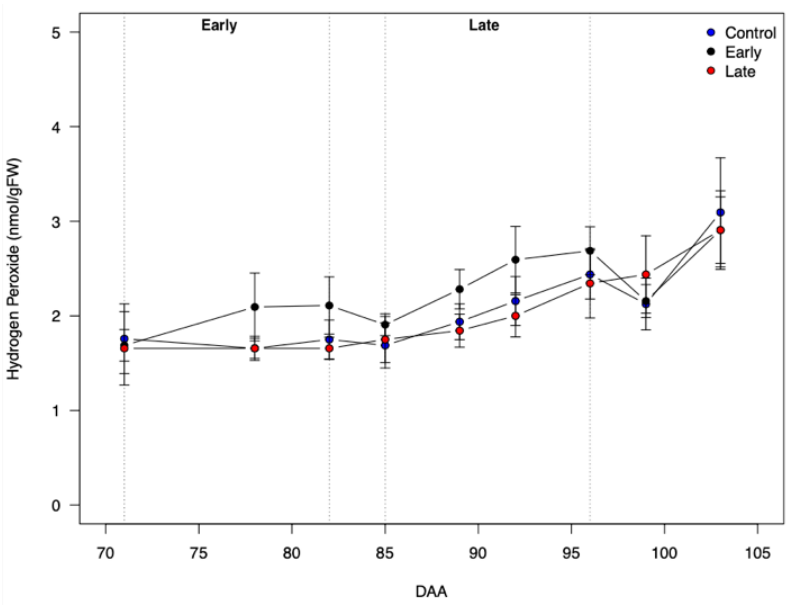


**Figure 9** Comparison of hydrogen peroxide means ± standard error, n = 20. One-Way ANOVA determined p>0.05 for all dates. A Piecewise linear regression model applied to this data did not establish significant breakpoints in rate of $H_2O_2$ accumulation. Vertical dashed lines indicate treatment periods. The early treatment spanned 71-82DAA and the late treatment spanned 85-96DAA.

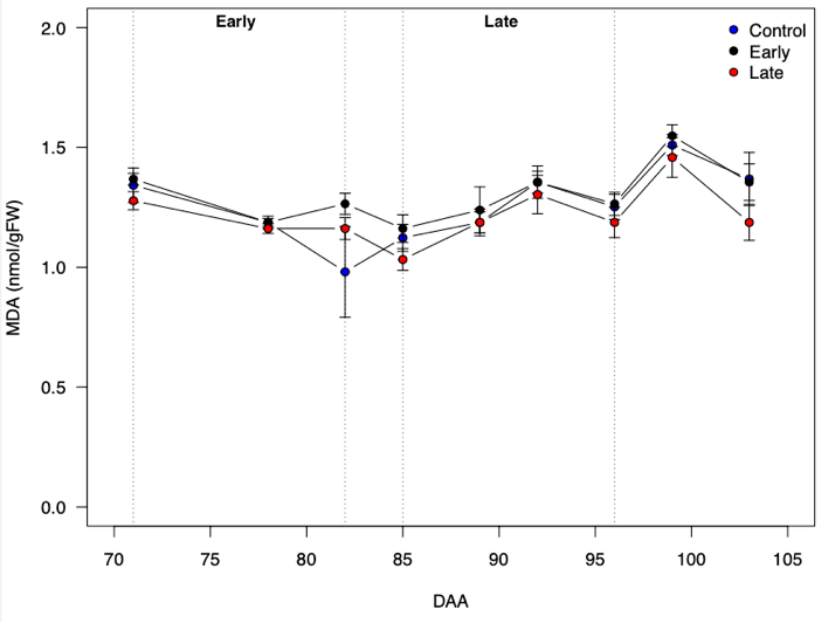


**Figure 10** Comparison of MDA means ± standard error by treatment, n = 20. One-Way ANOVA for each date determined p>0.05. Vertical dashed lines indicate treatment periods. The early treatment spanned 71-82DAA and the late treatment spanned 85-96DAA.

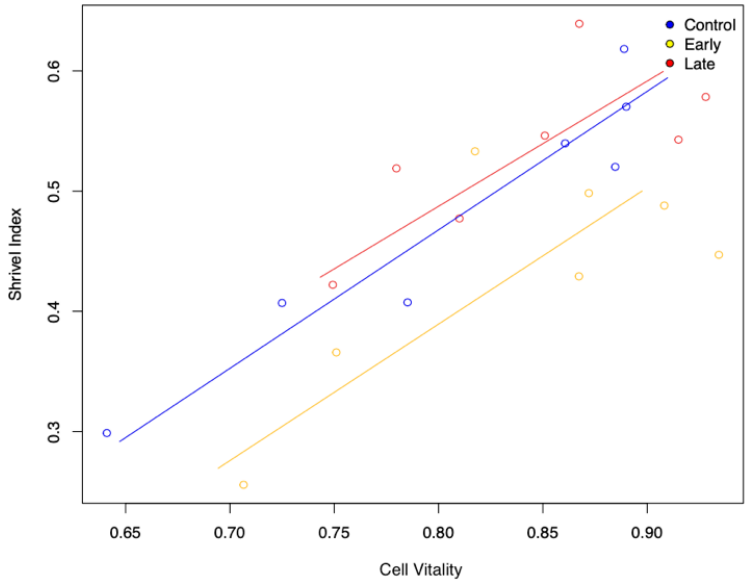


**Figure 11** SMATR correlation plot of %LT vs ShI. $R^2$ values for control, early and late treatments respectively are: 0.91 ($p<.05$) , 0.53 ($p>.05$), 0.53 ($p>05$). %Cell vitality was scaled to match the Shrivel Index scale.

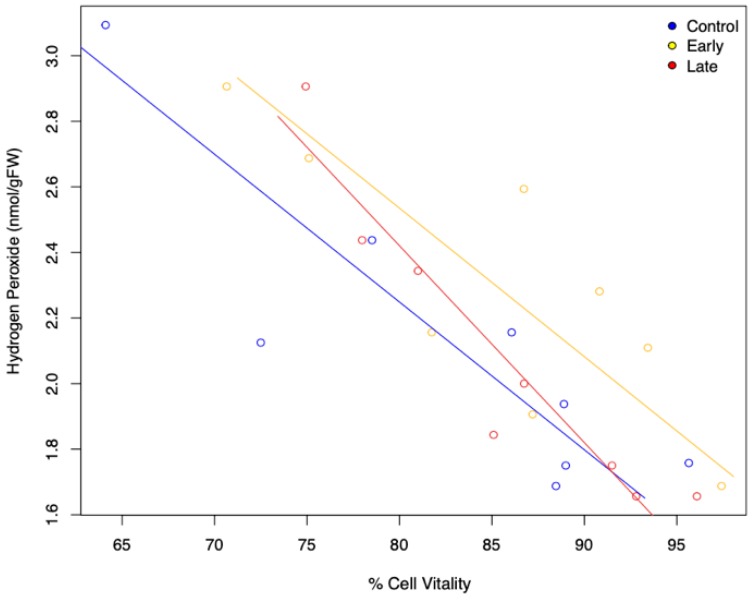


**Figure 12** SMATR correlation plot of %LT vs $H_2O_2$. $R^2$ values for control, early and late treatments respectively are: 0.77 ($p<.05$), 0.68 ($p<.05$), .89 ($p<.05$).

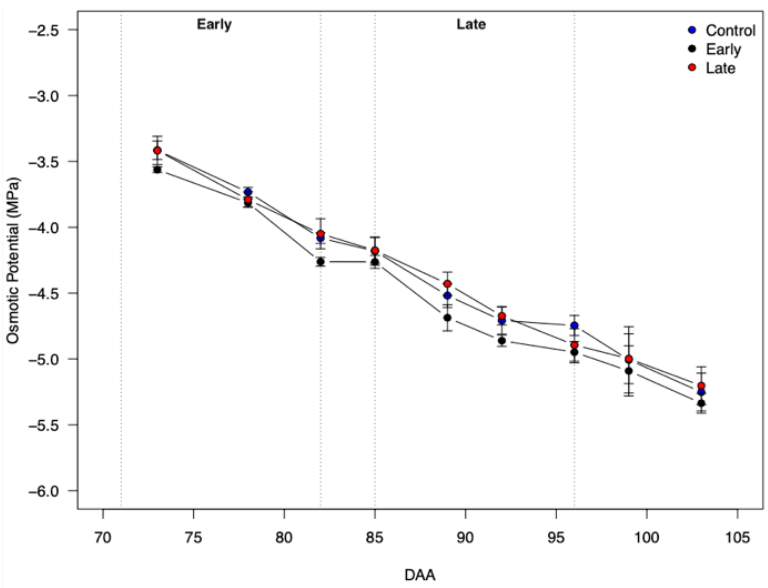


**Figure 13** Osmotic potential ± standard error means derived from composite vine samples. One-way ANOVA for the last date (at harvest) determined p>0.05. Vertical dashed lines indicate treatment periods. The early treatment spanned 71-82DAA, the late treatment spanned 85-96DAA.

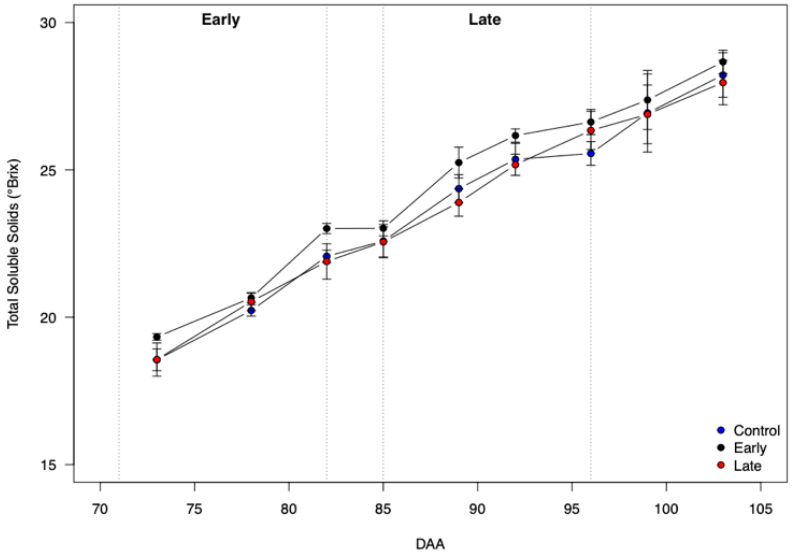


**Figure 14** Total Soluble Solids ± standard error means derived from a Osmotic Potential with a linear equation from Bonada et al. (2017). Vertical dashed lines indicate treatment periods. The early treatment spanned 71-82DAA and the late treatment spanned 85-96DAA.

# Tables

**Table 1** Midday and Predawn weekly mean water potentials ± standard error (MPa), n= 30. *P*-values were determined by one-way ANOVA.

| | | Midday | | | | Predawn | | | |
|---|---|---|---|---|---|---|---|---|---|
| Date | DAA | Control | Early | Late | *p*-value | Control | Early | Late | *p*-value |
| 28-Jul | 74 | -1.32 ± 0.046 | -1.45 ± 0.058 | -1.3 ± 0.033 | .07 | -0.56 ± 0.040 | -0.61 ± 0.053 | -0.54 ± 0.046 | .52 |
| 4-Aug | 81 | -1.32 ± 0.031 | -1.20 ± 0.041 | -1.29 ± 0.048 | .14 | -0.65 ± 0.051 | -0.69 ± 0.048 | -0.60 ± 0.062 | .50 |
| 11-Aug | 88 | -1.25 ± 0.041 | -1.20 ± 0.034 | -1.23 ± 0.062 | .77 | -0.40 ± 0.030 | -0.34 ± 0.03 | -0.46 ± 0.053 | .11 |
| 20-Aug | 97 | -1.27 ± 0.079 | -1.28 ± 0.047 | -1.26 ± 0.034 | .69 | -0.46 ± 0.028 | -0.47± 0.019 | -0.46 ± 0.046 | .99 |
| 25-Aug | 102 | -1.20 ± 0.040 | -1.18 ± 0.049 | -1.07 ± 0.05 | .16 | -0.52 ± 0.021 | -0.58 ± 0.024 | -0.52 ± 0.025 | .16 |

**Table 2** Stomatal conductance ($g_s$) and photosynthesis (A) rates ± standard error. Asterisks/boldface indicates a significant treatment effect on $g_s$ or A determined by one-way ANOVA and Tukey's HSD test.

| | | $g_s$ (mol $m^{-2}$ $s^{-1}$) | | | | A (µmol $m^{-2}$ $s^{-1}$) | | | |
|---|---|---|---|---|---|---|---|---|---|
| Date | DAA | Control | Early | Late | *p*-value | Control | Early | Late | *p*-value |
| 28-Jul | 74 | 0.18 ± 0.021 | 0.19 ± 0.015 | 0.26 ± 0.024* | **.02** | 13.8 ± 1.1 | 13.3 ± 0.7 | 16.7 ± 1.0* | **.03** |
| 4-Aug | 81 | 0.24 ± 0.021 | 0.24 ± 0.016 | 0.27 ± 0.019 | .36 | 15.5 ± 1.1 | 14.1 ± 0.7 | 16.7 ± 0.8 | .13 |
| 11-Aug | 88 | 0.18 ± 0.016 | 0.20 ± 0.016 | 0.20 ± 0.021 | .58 | 15.0 ± 0.9 | 14.4 ± 0.7 | 14.7 ± 0.7 | .86 |
| 20-Aug | 97 | 0.21 ± 0.022 | 0.21 ± 0.023 | 0.21 ± 0.014 | .99 | 12.0 ± 1.1 | 12.7 ± 0.9 | 11.7 ± 0.7 | .74 |
| 25-Aug | 102 | 0.19 ± 0.018 | 0.19 ± 0.019 | 0.22 ± 0.013 | .51 | 12.6 ± 0.8 | 11.4 ± 1.0 | 13.7 ± 0.9 | .24 |

**Table 3** Confidence intervals (95%) for breakpoints and pre-onset/post-onset slopes (m, m') in the piecewise linear regression model for Cell Death, $H_2O_2$ and Shrivel Index. Breakpoints are in terms of days after anthesis and slopes represent rate of declining %cell vitality / day after anthesis. Asterisks distinguish non-overlapping confidence intervals signifying significant treatment effects.

| | | Rate of Cell Death | | | Hydrogen Peroxide Accumulation | | | Shrivel Index | | |
|---|---|---|---|---|---|---|---|---|---|---|
| | Treatment | Slope/Breakpoint | CI_lower | CI_upper | Slope/Breakpoint | CI_lower | CI_upper | Slope/Breakpoint | CI_lower | CI_upper |
| m | 1 | -0.42 | -0.61 | -0.23 | -0.003 | -0.003 | 0.054 | 0.007 | -0.005 | 0.02 |
| | 2 | -0.46 | -1.36 | 0.44 | 0.026 | -0.065 | 0.118 | 0.02 | -0.031 | 0.071 |
| | 3 | -0.30 | -0.86 | 0.26 | 0.088 | -0.011 | 0.021 | 0.001 | -0.015 | 0.018 |
| Break-point | 1 | 92.4 | 89.3 | 95.5 | 85.9 | 74.7 | 97.2 | 89.0 | 83.7 | 94.3 |
| | 2 | 89.0 | 67.0 | 111 | 94.5 | 88.8 | 277.8 | 86.0 | 74.2 | 97.7 |
| | 3 | 83.3 | 73.0 | 93.6 | 87.9 | 84.69 | 91.2 | 92.0 | 79.5 | 104.5 |
| m' | 1 | -2.06 | -2.68* | -1.44* | 0.067 | 0.012 | 0.121 | 0.021 | -0.0338 | -0.008 |
| | 2 | -1.21 | -2.7 | 0.28 | 0.033 | -0.015 | 0.083 | -0.011 | -0.0336 | 0.011 |
| | 3 | -0.89 | -1.19* | -0.60* | 0.074 | 0.058 | 0.089 | -0.014 | -0.0307 | 0.002 |

**Table 4** Juice analysis of composite vine samples at harvest (103 DAA).

| Treatment | Brix | pH | TA (g/L) |
|---|---|---|---|
| Control | 26.7 ± 0.5 | 3.54 ± 0.03 | 6.16 ± 0.10 |
| Early | 27.1 ± 0.3 | 3.58 ± 0.03 | 6.04 ± 0.17 |
| Late | 25.6 ± 0.6 | 3.56 ± 0.02 | 6.00 ± 0.15 |
| p-value | .454 | .139 | .309 |

## References


Alston, J. M., K. B. Fuller, J. T. Lapsley and G. Soleas. 2011. Too much of a good thing? Causes and consequences of increases in sugar content of california wine grapes. Journal of Wine Economics 6: 135-159.

Baxter-Burrell, A., Z. Yang, P. S. Springer and J. Bailey-Serres. 2002. Ropgap4-dependent rop gtpase rheostat control of arabidopsis oxygen deprivation tolerance. Science 296: 2026-2028.

Berg, N. and A. Hall. 2017. Anthropogenic warming impacts on california snowpack during drought. Geophysical Research Letters 44: 2511-2518.

Bonada, M., V. Sadras, M. Moran and S. Fuentes. 2013a. Elevated temperature and water stress accelerate mesocarp cell death and shrivelling, and decouple sensory traits in shiraz berries. Irrigation Sci 31: 1317-1331.

Bonada, M., V. O. Sadras and S. Fuentes. 2013b. Effect of elevated temperature on the onset and rate of mesocarp cell death in berries of shiraz and chardonnay and its relationship with berry shrivel. Aust J Grape Wine R 19: 87-94.

Bondada, B. and M. Keller. 2012. Morphoanatomical symptomatology and osmotic behavior of grape berry shrivel. Journal of the American Society for Horticultural Science 137: 20-30.

Bondada, B. 2014. Structural and compositional characterization of suppression of uniform ripening in grapevine: A paradoxical ripening disorder of grape berries with no known causative clues. Journal of the American Society for Horticultural Science 139: 567-581.

Bondada, B., E. Harbertson, P. M. Shrestha and M. Keller. 2017. Temporal extension of ripening beyond its physiological limits imposes physical and osmotic challenges perturbing metabolism in grape berries. Sci Hortic-Amsterdam 219: 135-143.

Brodribb, T. J. 2009. Xylem hydraulic physiology: The functional backbone of terrestrial plant productivity. Plant Science 177: 245-251.

Cadot, Y., M. T. Miñana-Castelló and M. Chevalier. 2006. Anatomical, histological, and histochemical changes in grape seeds from vitis vinifera l. Cv cabernet franc during fruit development. J Agr Food Chem 54: 9206-9215.

California Department of Food and Agriculture (CDFA). (1975-2023). Grape Crush Report, Final 1975-2023. Retrieved from https://www.nass.usda.gov/Statistics_by_State/California/Publications/Specialty_and_Other_Releases/Grapes/Crush/Reports/index.php

Cao, S. F., Z. Y. Xiao, V. Jiranek and S. D. Tyerman. 2019. The VvBAP1 gene is identified as a potential inhibitor of cell death in grape berries. Funct Plant Biol 46: 428-442.

Castellarin, S. D., G. A. Gambetta, H. Wada, M. N. Krasnow, G. R. Cramer, E. Peterlunger, K. A. Shackel and M. A. Matthews. 2016. Characterization of major ripening events during softening in grape: Turgor, sugar accumulation, abscisic acid metabolism, colour development, and their relationship with growth. J Exp Bot 67: 709-722.

Carvalho, L. C., P. Vidigal and S. Amâncio. 2015. Oxidative stress homeostasis in grapevine. Front Env Sci-Switz 3:

Choat, B., G. A. Gambetta, K. A. Shackel and M. A. Matthews. 2009. Vascular function in grape berries across development and its relevance to apparent hydraulic isolation. Plant Physiol 151: 1677-1687.

Chou, H. C., K. Suklje, G. Antalick, L. M. Schmidtke and J. W. Blackman. 2018. Late-season shiraz berry dehydration that alters composition and sensory traits of wine. J Agr Food Chem 66: 7750-7757.

Claverie, M., P. Lecomte, G. Delorme, V. Dumot, O. Jacquet and H. Cochard. 2023. Xylem water transport is influenced by age and winter pruning characteristics in grapevine (vitis vinifera). OENO One 57: 53-68.

Cook, B. I. and E. M. Wolkovich. 2016. Climate change decouples drought from early wine grape harvests in france. Nature Climate Change 6: 715-719.

Coombe, B. and P. Matile. 1980. Solute accumulation by grape pericarp cells. I. Sugar uptake by skin, segments. Biochemie und Physiologie der Pflanzen 175: 369-381.

De Pinto, M. C., V. Locato and L. De Gara. 2012. Redox regulation in plant programmed cell death. Plant Cell Environ 35: 234-244.

Evert, R. F. 1982. Sieve-tube structure in relation to function. Bioscience 32: 789-795.

Famiani, F., D. Farinelli, A. Palliotti, S. Moscatello, A. Battistelli and R. P. Walker. 2014. Is stored malate the quantitatively most important substrate utilised by respiration and ethanolic fermentation in grape berry pericarp during ripening? Plant Physiol Bioch 76: 52-57.

Fuentes, S., W. Sullivan, J. Tilbrook and S. Tyerman. 2010. A novel analysis of grapevine berry tissue demonstrates a variety-dependent correlation between tissue vitality and berry shrivel. Aust J Grape Wine R 16: 327-336.

Fukao, T. and J. Bailey-Serres. 2004. Plant responses to hypoxia–is survival a balancing act? Trends Plant Sci 9: 449-456.

Fyfe, J. C., C. Derksen, L. Mudryk, G. M. Flato, B. D. Santer, N. C. Swart, N. P. Molotch, X. Zhang, H. Wan and V. K. Arora. 2017. Large near-term projected snowpack loss over the western united states. Nature communications 8: 14996.

Gambetta, G., C. Manuck, S. Drucker, T. Shaghasi, K. Fort, M. Matthews, M. Walker and A. Mcelrone. 2012. The relationship between root hydraulics and scion vigour across vitis rootstocks: What role do root aquaporins play? J Exp Bot 63: 6445-6455.

Gechev, T. S., F. Van Breusegem, J. M. Stone, I. Denev and C. Laloi. 2006. Reactive oxygen species as signals that modulate plant stress responses and programmed cell death. Bioessays 28: 1091-1101.

Gershunov, A. and K. Guirguis. 2012. California heat waves in the present and future. Geophysical Research Letters 39:

Girona, J., M. Mata, J. Del Campo, A. Arbonés, E. Bartra and J. Marsal. 2006. The use of midday leaf water potential for scheduling deficit irrigation in vineyards. Irrigation Sci 24: 115-127.

Gowder Shekharappa, C. 2022. The role of gamma-aminobutyric acid and hydrogen peroxide in cell death in grape berry development, Thesis. University of Adelaide.

Gu, T., Y. Han, R. Huang, R. J. Mcavoy and Y. Li. 2016. Identification and characterization of histone lysine methylation modifiers in fragaria vesca. Scientific Reports 6: 23581.

Harris, J., P. Kriedemann and J. Possingham. 1971. Grape berry respiration: Effects of metabolic inhibitors. Vitis 9: 291-298.

Hodges, D. M., J. M. Delong, C. F. Forney and R. K. Prange. 1999. Improving the thiobarbituric acid-reactive-substances assay for estimating lipid peroxidation in plant tissues containing anthocyanin and other interfering compounds. Planta 207: 604-611.

Jimenez, A., G. Creissen, B. Kular, J. Firmin, S. Robinson, M. Verhoeyen and P. Mullineaux. 2002. Changes in oxidative processes and components of the antioxidant system during tomato fruit ripening. Planta 214: 751-758.

Keller, M. 2010. Managing grapevines to optimise fruit development in a challenging environment: A climate change primer for viticulturists. Aust J Grape Wine R 16: 56-69.

Keller, M., P. Romero, H. Gohil, R. P. Smithyman, W. R. Riley, L. F. Casassa and J. F. Harbertson. 2016. Deficit irrigation alters grapevine growth, physiology, and fruit microclimate. Am J Enol Viticult 67: 426-435.

Keller, M., J. P. Smith and B. R. Bondada. 2006. Ripening grape berries remain hydraulically connected to the shoot. J Exp Bot 57: 2577-2587.

Keller, M., Y. Zhang, P. M. Shrestha, M. Biondi and B. R. Bondada. 2015. Sugar demand of ripening grape berries leads to recycling of surplus phloem water via the xylem. Plant Cell Environ 38: 1048-1059.

Kennedy, J. A., G. J. Troup, J. R. Pilbrow, D. R. Hutton, D. Hewitt, C. R. Hunter, R. Ristic, P. G. Iland and G. P. Jones. 2000. Development of seed polyphenols in berries from vitis vinifera l. Cv. Shiraz. Aust J Grape Wine R 6: 244-254.

Knipfer, T., J. Fei, G. A. Gambetta, A. J. Mcelrone, K. A. Shackel and M. A. Matthews. 2015. Water transport properties of the grape pedicel during fruit development: Insights into xylem anatomy and function using microtomography. Plant Physiol 168: 1590-1602.

Krasnow, M., M. Matthews and K. Shackel. 2008. Evidence for substantial maintenance of membrane integrity and cell viability in normally developing grape berries throughout development. J Exp Bot 59: 849-859.

Levine, A., R. Tenhaken, R. Dixon and C. Lamb. 1994. H2o2 from the oxidative burst orchestrates the plant hypersensitive disease resistance response. Cell 79: 583-593.

Liu, H.-N., Y.-T. Wan, Y.-H. Yu and D.-L. Guo. 2021. Identification of grape h3k4 genes and their expression profiles during grape fruit ripening and postharvest ros treatment. Genomics 113: 3793-3803.

Livneh, B., T. J. Bohn, D. W. Pierce, F. Munoz-Arriola, B. Nijssen, R. Vose, D. R. Cayan and L. Brekke. 2015. A spatially comprehensive, hydrometeorological data set for mexico, the us, and southern canada 1950-2013. Sci Data 2:

Mansoor, S., O. A. Wani, J. K. Lone, S. Manhas, N. Kour, P. Alam, A. Ahmad and P. Ahmad. 2022. Reactive oxygen species in plants: From source to sink. Antioxidants-Basel 11:

Matthews, M. A., G. Cheng and S. A. Weinbaum. 1987. Changes in water potential and dermal extensibility during grape berry development. Journal of the American Society for Horticultural Science 112: 314-319.

Mendez, M. P., L. Sanchez and N. Dokoozlian. 2011. Crop load and irrigation management during the latter stages of ripening: Effects on vine water status, fruit dehydration and fruit composition of 'merlot' grapevines. Acta Hortic 889: 67-74.

Minio, A., M. Massonnet, R. Figueroa-Balderas, A. M. Vondras, B. Blanco-Ulate and D. Cantu. 2019. Iso-seq allows genome-independent transcriptome profiling of grape berry development. G3-Genes Genom Genet 9: 755-767.

Morales, M. and S. Munné-Bosch. 2019. Malondialdehyde: Facts and artifacts. Plant Physiol 180: 1246-1250.

Neill, S., R. Desikan and J. Hancock. 2002. Hydrogen peroxide signalling. Current opinion in plant biology 5: 388-395.

Netzer, Y., S. Munitz, I. Shtein and A. Schwartz. 2019. Structural memory in grapevines: Early season water availability affects late season drought stress severity. European Journal of Agronomy 105: 96-103.

Peacock B, Williams LE, Christensen P. 1998. Water management irrigation scheduling. *University of California Cooperative Extension* Pub.IG9-98.

Petrov, V. D. and F. Van Breusegem. 2012. Hydrogen peroxide—a central hub for information flow in plant cells. AoB plants 2012: pls014.

Pilati, S., D. Brazzale, G. Guella, A. Milli, C. Ruberti, F. Biasioli, M. Zottini and C. Moser. 2014. The onset of grapevine berry ripening is characterized by ros accumulation and lipoxygenase-mediated membrane peroxidation in the skin. Bmc Plant Biol 14:

Pilati, S., M. Perazzolli, A. Malossini, A. Cestaro, L. Dematté, P. Fontana, A. Dal Ri, R. Viola, R. Velasco and C. Moser. 2007. Genome-wide transcriptional analysis of grapevine berry ripening reveals a set of genes similarly modulated during three seasons and the occurrence of an oxidative burst at veraison. Bmc Genomics 8:

Rasmussen, D. J., M. Meinshausen and R. E. Kopp. 2016. Probability-weighted ensembles of us county-level climate projections for climate risk analysis. J Appl Meteorol Clim 55: 2301-2322.

Reimers, H., B. Steinberg and W. Kiefer. 1994. Ergebnisse von wurzeluntersuchungen an reben bei offenem und begrüntem boden. Wein-Wissenschaft 49: 136-145.

Ristic, R. and P. G. Iland. 2005. Relationships between seed and berry development of vitis vinifera l. Cv shiraz: Developmental changes in seed morphology and phenolic composition. Aust J Grape Wine R 11: 43-58.

Rogiers, S. Y. and B. P. Holzapfel. 2015. The plasticity of berry shrivelling in 'shiraz': A vineyard survey. Vitis 54: 1-8.

Ruffner, H. 1982. Metabolism of tartaric and malic acids in vitis v a review. A. Vitis-,: 247V259

Sadras, V. O., M. A. Moran and M. Bonada. 2013. Effects of elevated temperature in grapevine. I berry sensory traits. Aust J Grape Wine R 19: 95-106.

Shivashankara, K., R. Laxman, G. Geetha, T. Roy, N. Srinivasa Rao and V. Patil. 2013. Volatile aroma and antioxidant quality of ‘shiraz’grapes at different stages of ripening. International Journal of Fruit Science 13: 389-399.

Suklje, K., X. Y. Zhang, G. Antalick, A. C. Clark, A. Deloire and L. M. Schmidtke. 2016. Berry shriveling significantly alters shiraz grape and wine chemical composition. J Agr Food Chem 64: 870-880.

Sun, Q., T. L. Rost and M. A. Matthews. 2008. Wound-induced vascular occlusions in vitis vinifera (vitaceae): Tyloses in summer and gels in winter1. American Journal of Botany 95: 1498-1505.

Sun, Q., Y. Sun, M. A. Walker and J. M. Labavitch. 2013. Vascular occlusions in grapevines with pierce's disease make disease symptom development worse. Plant Physiol 161: 1529-1541.

Sun, J., X. R. You, L. Li, H. X. Peng, W. Q. Su, C. B. Li, Q. G. He and F. Liao. 2011. Effects of a phospholipase d inhibitor on postharvest enzymatic browning and oxidative stress of litchi fruit. Postharvest Biol Tec 62: 288-294.

Swain, D. L., B. Langenbrunner, J. D. Neelin and A. Hall. 2018. Increasing precipitation volatility in twenty-first-century california. Nature Climate Change 8: 427-433.

Sweetman, C., D. C. Wong, C. M. Ford and D. P. Drew. 2012. Transcriptome analysis at four developmental stages of grape berry (vitis vinifera cv. Shiraz) provides insights into regulated and coordinated gene expression. Bmc Genomics 13: 1-25.

Tagnon, M. D. and K. O. Simeon. 2017. Aldehyde dehydrogenases may modulate signaling by lipid peroxidation-derived bioactive aldehydes. Plant signaling & behavior 12: e1387707.

Terrier, N. and C. Romieu. 2001. Grape Berry Acidity. In Molecular Biology and Biotechnology of the Grapevine. Roubelakis-Angelakis KA (ed.), pp. 35-57. Springer Dordrecht, Germany.

Tilbrook, J. and S. D. Tyerman. 2008. Cell death in grape berries: Varietal differences linked to xylem pressure and berry weight loss. Funct Plant Biol 35: 173-184.

Tilbrook, J. and S. D. Tyerman. 2009. Hydraulic connection of grape berries to the vine: Varietal differences in water conductance into and out of berries, and potential for backflow. Funct Plant Biol 36: 541-550.

Triantaphylidès, C. and M. Havaux. 2009. Singlet oxygen in plants: Production, detoxification and signaling. Trends Plant Sci 14: 219-228.

Valandro, F., P. K. Menguer, C. Cabreira-Cagliari, M. Margis-Pinheiro and A. Cagliari. 2020. Programmed cell death (pcd) control in plants: New insights from the deathosome. Plant Sci 299:

Webb, L., P. Whetton, J. Bhend, R. Darbyshire, P. Briggs and E. Barlow. 2012. Earlier wine-grape ripening driven by climatic warming and drying and management practices. Nature Climate Change 2: 259-264.

Williams LE. 2010. Interaction of rootstock and applied water amounts at various fractions of estimated evapotranspiration (ETc) on productivity of Cabernet Sauvignon: Effects of rootstock and water amounts on yield. *Australian Journal of Grape and Wine Research* 16: 434–444.

Wilson, T. S., B. M. Sleeter and D. R. Cameron. 2016. Future land-use related water demand in california. Environ Res Lett 11:

Xi, F. F., L. L. Guo, Y. H. Yu, Y. Wang, Q. Li, H. L. Zhao, G. H. Zhang and D. L. Guo. 2017. Comparison of reactive oxygen species metabolism during grape berry development between 'kyoho' and its early ripening bud mutant 'fengzao'. Plant Physiol Bioch 118: 634-642.

Xiao, Z., S. Liao, S. Y. Rogiers, V. O. Sadras and S. D. Tyerman. 2018a. Effect of water stress and elevated temperature on hypoxia and cell death in the mesocarp of shiraz berries. Aust J Grape Wine R 24: 487-497.

Xiao, Z. Y., S. Y. Rogiers, V. O. Sadras and S. D. Tyerman. 2018b. Hypoxia in grape berries: The role of seed respiration and lenticels on the berry pedicel and the possible link to cell death. J Exp Bot 69: 2071-2083.

Zhao, J., T. D. Missihoun and D. Bartels. 2018. The ataf1 transcription factor is a key regulator of aldehyde dehydrogenase 7b4 (aldh7b4) gene expression in arabidopsis thaliana. Planta 248: 1017-1027.

Zhang, X. Y., X. L. Wang, X. F. Wang, G. H. Xia, Q. H. Pan, R. C. Fan, F. Q. Wu, X. C. Yu and D. P. Zhang. 2006. A shift of phloem unloading from symplasmic to apoplasmic pathway is involved in developmental onset of ripening in grape berry. Plant Physiol 142: 220-232.